

Characterization of mono- and diphasic mullite precursor powders prepared by aqueous routes. ^{27}Al and ^{29}Si MAS-NMR spectroscopy investigations

I. JAYMES, A. DOUY, D. MASSIOT, J. P. COUTURES

CNRS-Centre de Recherches sur la Physique des Hautes Températures, 1D, Avenue de la Recherche Scientifique, 45071 Orléans Cedex 02, France

The structural evolution from amorphous to crystalline mullite, for different $3\text{Al}_2\text{O}_3 \cdot 2\text{SiO}_2$ mono- and diphasic precursors, has been investigated by ^{29}Si and ^{27}Al magic angle spinning nuclear magnetic resonance (MAS NMR) spectroscopy. The crystallization has also been studied by X-ray diffraction (XRD) and differential scanning calorimetry (DSC). The chemical composition in the aluminosilicate network of the diphasic precursors and in the crystallized phases has been determined from the ^{29}Si NMR spectra. A close agreement is found with the composition deduced from the lattice parameters measured by XRD. For monophasic precursors the amount of hexa-coordinated aluminium atoms decreases when the temperature increases while Al(IV) and Al(V) increase. Al(VI) practically completely disappears just before the crystallization at 980°C . An alumina-rich mullite $2\text{Al}_2\text{O}_3 \cdot \text{SiO}_2$ (2:1 mullite) is then formed through a strong exotherm. An enthalpy of 75 kJ per mol is determined for the crystallization of the 2:1 mullite. At higher temperatures the segregated silica is progressively reincorporated into the mullite lattice. For diphasic precursors the ^{29}Si NMR spectroscopy shows the segregation of silica. The aluminosilicate network is then richer in alumina and the amount of remaining AlO_6 octahedra before the crystallization at 980°C is higher. Spinel crystallizes and continues to become richer in alumina until it reacts with silica to form the stoichiometric 3:2 mullite at $1260\text{--}1275^\circ\text{C}$. The nature of the crystallization is related to the local composition of the amorphous aluminosilicate network and to the amount of AlO_6 octahedra on approaching 980°C .

1. Introduction

Mullite is the only high temperature stable crystalline phase in the aluminosilicate system ($\text{Al}_2\text{O}_3\text{--SiO}_2$) under normal pressure. It has been the subject of considerable interest in recent years, due to its excellent properties, such as high temperature strength and creep resistance, good thermal and chemical stability, low thermal expansion coefficient, good dielectric properties and infrared transparency [1]. The synthesis of mullite ($3\text{Al}_2\text{O}_3 \cdot 2\text{SiO}_2$) using a large number of chemical precursor combinations and processes has been reported [2]. The precursors obtained by wet chemical processes have been classified either as single phase and diphasic [3], or as type I, type II or type III [4]. When the chemical homogeneity is at the molecular level, for monophasic or type I precursors such as polymeric gels, mullite rapidly crystallizes through a strong exotherm at about 980°C . On the other hand, when the chemical homogeneity is at the nanometre scale, with diphasic or type III precursors, mullite formation is usually preceded by the weak crystalliza-

tion of transient alumina phases, such as cubic Al-Spinel or $\gamma\text{-Al}_2\text{O}_3$, and occurs only at higher temperatures through a second exothermic reaction at about 1250°C .

Progress in the synthesis of chemically homogeneous multicomponent oxides is particularly indebted to sol-gel science [5, 6] essentially because of a better knowledge of metal alkoxides chemistry. However it is well known that the hydrolysis and polycondensation of silicon alkoxides are very low compared to those of aluminium, and so great care has to be taken to achieve a homogeneous co-polymerization. This may be reached by very slow hydrolysis [7, 8], by prehydrolysis, at least partially, of the silicon alkoxide [8] or by modifying the aluminium alkoxide by a chelating group (for example, acetylacetonate) to reduce its reactivity [9–11]. In all cases the experimental conditions have to be strictly controlled: slow hydrolysis, quantity of added water for hydrolysis, pH of catalysis, solvent and temperature. The formation of mullite at 980°C has been more easily achieved from mixtures of

one chloride and one alkoxide [12] or when the more reactive of the alkoxides is replaced by a hydrated salt, aluminium nitrate nonahydrate, in combination with tetraethoxysilane in absolute ethanol [3,13–17]. However, it is still important to avoid rapid hydrolysis since additional water, basic conditions or insufficient time for co-hydrolysis will result in a heterogeneity that produces spinel nucleation [16].

In the present work, five different mullite precursor powders, obtained by different aqueous routes, have been studied. For each preparation a silicon alkoxide has been rapidly hydrolysed in a dilute aqueous solution of an aluminium salt. For three of these powders complete crystallization of mullite is obtained at a low temperature ($< 1000^\circ\text{C}$) whilst, for the other two the formation of mullite is retarded to higher temperatures. The structural evolution with temperature has been studied by differential scanning calorimetry (DSC), X-ray diffraction (XRD) and ^{27}Al and ^{29}Si magic angle spinning nuclear magnetic resonance (MAS-NMR) spectroscopy.

2. Experimental procedure

2.1. Sample preparation

Two mullite precursor powders were prepared by an organic gel-assisted process [18,19]. For the first sample, powder A, aluminium nitrate ($\text{Al}(\text{NO}_3)_3 \cdot 9\text{H}_2\text{O}$) was dissolved in water. The aluminium cations were then chelated by citric acid (one citric acid per nitrate ion), and ammonia was added to adjust the pH to ~ 2 as for the nitrate solution. Silicon was introduced as 3-triethoxysilyl-propylamine ($\text{C}_2\text{H}_5\text{O}$)₃ Si(CH₂)₃NH₂ (TESPA) under strong stirring. This alkoxide was rapidly hydrolysed and a clear solution was obtained. This solution was easily gelled by *in situ* formation of a polyacrylamide network. For this, the organic monomers, acrylamide and N, N'-methylene diacrylamide, were dissolved and co-polymerized by adding α , α' -azoisobutyronitrile as a radical polymerization initiator at 80°C . The aqueous gel was transformed into a meringue in a microwave oven and calcined to 750°C (4 h) at a heating rate of 2°C per min in a ventilated furnace.

For the second sample, powder B, tetraethoxysilane Si(C₂H₅O)₄ (TEOS) was hydrolysed under strong stirring in a 0.6 M aqueous solution of aluminium nitrate. Urea was introduced (10 urea moles per Al nitrate mole) and the solution was gelled by polyacrylamide. The gel was stored at 95°C for 15 h and then calcined to 750°C .

Two other powders were obtained by spray-drying aqueous solutions [20]. TEOS was hydrolysed in a solution of aluminium nitrate. The freshly prepared clear solution was spray dried using a laboratory apparatus (Büchi, Flawil, Switzerland, 190 mini spray-drier equipped with a 0.5 mm nozzle) with compressed air preheated to 200°C . The resulting powder was then heat-treated to various temperatures (powder C). For powder D, the diluted aqueous precursor solution was aged at 100°C for 3 days, becoming opalescent, before being spray dried and heat-treated like powder C.

The precursor E was obtained by homogeneous precipitation [21]. For this, urea (1.8 mole per mole of aluminium nitrate) was added to a freshly prepared solution of aluminium nitrate and silicic acid. This solution was stored at 90°C , transforming into a gel, then slowly into a clear colloidal sol and finally into a second gel. This gel was filtered, washed with de-ionized water and dried at 100°C before being heat-treated.

2.2. Characterization

High resolution solid state ^{27}Al and ^{29}Si MAS-NMR spectra were obtained on a Bruker MSL-300 spectrometer (Bruker, Karlsruhe, Germany), operating at a magnetic field strength of 7.04 T, and spinning the samples at the magic angle ($54^\circ 44'$). The Larmor frequencies corresponding to ^{27}Al and ^{29}Si were respectively 78.2 and 59.6 MHz. The samples were contained in zirconia rotors of 7 mm diameter for the silicon and 4 mm for the aluminium.

The ^{27}Al NMR experiments were recorded using a pulse length of 1 μs , with a recycle time of 1 s. The spectral width used (SW) was 1 MHz, with a spectral size (SI) of 8 K and a time domain (TD) or number of acquired points of 4 K. About 2000 accumulated scans were necessary to obtain a good signal to noise ratio for amorphous samples, but only 200 for crystallized samples. The spectra were obtained at room temperature with a spinning rate of 15 kHz, using a Bruker MAS probe. $\text{Al}(\text{NO}_3)_3/\text{HNO}_3$ was used as an external reference. The isotropic chemical shift positions and the estimated minimum quadrupolar frequencies were measured using central and satellite transitions as proposed by Jäger [22] and by Massiot *et al.* [23].

For the ^{29}Si NMR spectra 2 μs were used as a pulse length, with recycle time of 10 s; this relatively short time was permitted by an enrichment in gadolinium (0.04 wt % Gd₂O₃). The spectral width used was 0.5 MHz, with a spectral size and a time domain of 2 K. About 5500 scans were necessary to obtain a correct signal. The spinning rate used was 4 kHz and the chemical shifts are referenced to tetramethylsilane.

The differential scanning calorimetry (DSC) experiments (Setaram, Lyon, France) have been carried out at 5°C per min, under an oxygen atmosphere up to 1300°C , using alumina powder as a standard. X-ray powder diffraction (Philips PW1729 diffractometer, Eindhoven, The Netherlands), patterns using CuK_α radiation, were taken to characterize the crystallinity of the powders heated to different temperatures.

3. Results and discussion

3.1. Powder preparations

All the powders are obtained from relatively dilute aqueous solutions. The silicon alkoxides are hydrolysed in solutions of aluminium salts without added alcohol. The molar ratio water: alkoxide is $\sim 250:1$, so there is no problem concerning the pH, the quantity and the rate of water addition for the hydrolysis.

The precursor powders A and B are prepared with the aid of an organic network of polyacrylamide gel [24]. For powder A, aluminium is chelated by citric acid whilst the silicon alkoxide, TESPA, is broken into 3-trihydroxysilyl-propylamine $(\text{HO})_3\text{Si}(\text{CH}_2)_3\text{NH}_2$ which will further condense by the silanol groups, the carbon-silicon bond being hydrolysed only by heat treatment. The aqueous gel contains much water and organic species. The powder obtained after burning off all the organic residues is white, aggregated into thin platelets, with a high specific surface area ($280\text{ m}^2\text{ g}^{-1}$).

For powder B, TEOS is hydrolysed into silicic acid $\text{Si}(\text{OH})_4$ in an aqueous acidic solution of aluminium nitrate. The precursor powder results here from an homogeneous precipitation reaction [25–27] within the pores of the organic gel. By storing at 95°C , each mole of urea is hydrolysed into one mole of carbon dioxide and two moles of ammonia [28]. Globally this results in a slow and homogeneous addition of ammonia. Aluminium is precipitated as hydroxide while the raising of the pH to neutrality accelerates the condensation of silicic acid into silica gel [29]. After calcination to 750°C , the powder is white and also has a large specific surface area ($270\text{ m}^2\text{ g}^{-1}$).

Precursor E is also obtained by homogeneous precipitation, but without an organic gel, and more slowly, the amount of added urea as the base generator being smaller. A detailed study of the reaction by chemical analysis, dynamic light scattering and ^{29}Si and ^{27}Al NMR spectroscopy [30] has shown that, while the pH remains practically unchanged, a silica gel is rapidly formed at the beginning of the reaction. This gel is then slowly digested by partially hydrolysed aluminium species which break the Si–O–Si bonds and link to the gel by Si–O–Al bonds. Progressively a clear colloidal sol is obtained. When the hydrolysis of aluminum is nearly complete, a final gel precursor of mullite is obtained. This gel may be filtered and washed to eliminate the ammonium nitrate formed. This is not possible for the powder B preparation where the gel is made within the pores of an organic network. The dried gel is chemically very homogeneous, with a protoimogolite-like local structure and a single environment for the silicon atoms characterized by a NMR band at -78 ppm [31]. The specific surface area is high ($220\text{ m}^2\text{ g}^{-1}$).

Powders C and D are obtained by spray-drying aqueous solutions or sols also made by hydrolysing TEOS in a solution of aluminium nitrate. Powder C results from the transformation of the freshly prepared solution while for powder D the solution has been aged for 3 days at 100°C , becoming opalescent, before being sprayed. The aluminium nitrate being only partially decomposed by just spray drying, the powders are hygroscopic and have to be calcined to completely decompose the salt. They are made of inhomogeneously sized spherical and hollow particles [20], with a mean size of $2\text{--}10\text{ }\mu\text{m}$ typical of powders prepared by such a technique. The specific surface areas are very low compared to those of powders A and B $1.5\text{--}3\text{ m}^2\text{ g}^{-1}$ for the as-spray dried powders or fired to 500°C .

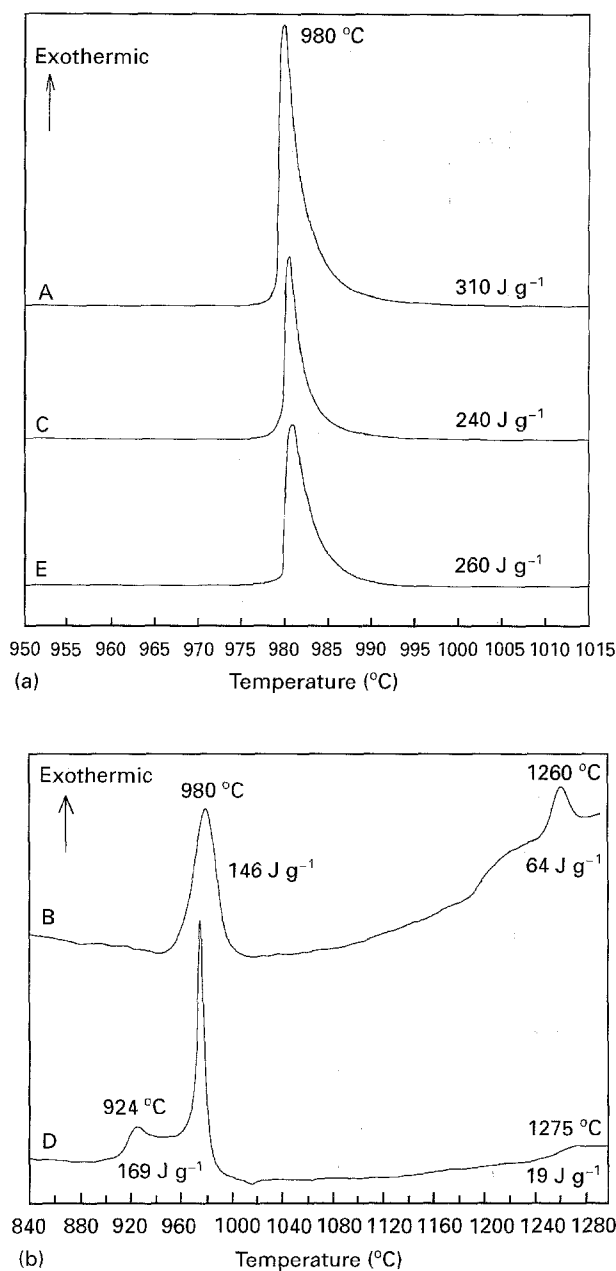


Figure 1 DSC curves of (a) monophasic (A, C and E) and (b) diphasic (B and D) precursors; heating rate: 10°C per min .

3.2. Structural evolution

The crystallization of the amorphous powders has been studied by DSC at a heating rate of 5°C per min , and the resulting crystalline phases identified by X-ray diffraction.

The DSC traces are shown on Fig. 1 (a and b). They are classified into two groups. For the first one (samples A, C and E) there is a single and strong exotherm at 980°C , and the enthalpy of the reaction is high ($240\text{--}310\text{ J g}^{-1}$) compared to the limited data in the literature (85 J g^{-1} estimated from DTA [3]). These precursors completely crystallize into mullite through the exothermic reaction. However the compositions of the resulting mullites are richer in alumina than the amorphous precursors. Mullite exists as a solid solution with the general formula $\text{Al}_{4+2x}\text{Si}_{2-2x}\text{O}_{10-x}$ where x represents the number of oxygen vacancies per unit cell, ranging generally from ~ 0.2 to 0.6 [32].

Recently a mullite with a 0.825 value for x has been described [33]. Cameron [32] and more recently Klug *et al.* [34] and Ban and Okada [35] have studied the variations of the unit cell dimensions in the solid solution range, and reported that a - and c -parameters of the orthorhombic cell increase with the x value, i.e., with the Al_2O_3 content while the b -parameter, slightly higher than a , decreases. It has been reported that the direct crystallization of amorphous $3\text{Al}_2\text{O}_3 \cdot 2\text{SiO}_2$ powders yields mullites richer in alumina than the stoichiometric 3:2 mullite. These mullites have often been called tetragonal or pseudo-tetragonal mullites, due to the lack of splitting for the (120) and (210) XRD doublet reflection [36]. The cell parameters have been determined for the samples A, C and E, heated to 1000 °C, and the compositions, deduced from Cameron's relation, are respectively 67.0, 67.2 and 66.6 mol%. These compositions are very close to that of 2:1 mullite (66.7 mol% Al_2O_3). The 2:1 mullite is also the compound which usually crystallizes from the melt. There is a similarity in the crystallization from the melt and from homogeneous amorphous precursors. Since it is the 2:1 mullite which crystallizes at 980 °C, an enthalpy of crystallization of $\sim 75 \text{ kJ mol}^{-1}$ is found for the 2:1 mullite. The crystallized phase, having a higher alumina content, coexists with some amorphous silica expelled from the network during the reaction. This free silica is progressively re-incorporated into the mullite network by further heating. At $\sim 1300 \text{ °C}$ the 3:2 composition is obtained.

The DSC curves of the two other precursors, B and D (Fig. 1) are different. For powder B there is also a strong exotherm at 980 °C, however of lower intensity (146 J g^{-1}) and a second exotherm at 1260 °C (64 J g^{-1}). The sample is amorphous until the first exotherm. After this point an XRD pattern displays only weakly crystallized aluminosilicate spinel peaks. The second exotherm corresponds to the transformation of this spinel phase into orthorhombic mullite. For powder D, prepared from a sol aged for 3 days at 100 °C before being spray-dried, there are two low temperature exotherms at 924 °C and 975 °C (170 J g^{-1} for the two peaks) and a third weaker one, at 1275 °C. After the first one there is only a weakly crystallized phase, Al₂Si spinel or $\gamma\text{-Al}_2\text{O}_3$. After the second peak at approximately the same temperature as for the other powders, the XRD diagram is not very different. It is still characteristic of a transient alumina phase with however a trace of mullite ($2\theta = 26.3^\circ$). The third peak at 1275 °C corresponds to the crystallization of the orthorhombic mullite.

The powders studied in this work present different structural evolutions. Precursors A, C and E are very homogeneous and crystallize completely into an alumina-rich mullite (2:1 mullite) at low temperature, with a high enthalpy reaction. For the powder B there is also a sharp and rather strong exotherm. Thus this powder presents a good level of homogeneity although the scale of heterogeneity must be just too high for a direct crystallization into mullite. This sample is obtained by homogeneous precipitation, as for the xerogel E, but entrapped in a network of polyacrylam-

ide gel. The difference in the crystallization behaviour of the two precursors is due to the presence of a high amount of ammonium nitrate, not eliminated in the case of the preparation with the organic gel. This has been confirmed by other experiments [21].

Powder C has the same behaviour as the mullite precursor powder spray-pyrolysed at 650 °C by Kanzaki *et al.* [37] from a solution made by dissolving aluminium nitrate and TEOS in a mixture of methanol and water. By ageing the precursor solution (D) there is no reaction between the aluminated and silicated species but only a polycondensation of silicic acid. The ageing of the precursor solution may thus be a convenient way to control the chemical heterogeneity in the spray-dried powders.

3.3. ^{29}Si and ^{27}Al MAS NMR spectroscopy

The structural evaluations for the different precursors, from the amorphous state to the well crystallized orthorhombic mullite, has been followed by investigating the local environments around Si and Al nuclei by MAS NMR spectroscopy (Fig. 2(a–j))

Aluminium has a quadrupolar nucleus (spin 5/2) and thus quadrupolar interactions, generating a number of inherent complexities [38]. Firstly, the chemical shift is affected by the second-order terms of the quadrupolar interaction. The observed chemical shift is not the true shift in the absence of quadrupolar effects, and depends on the operating magnetic field [39, 40]. Secondly, the resonance bands may be considerably broadened by the quadrupolar interaction and may even disappear in the background noise of the spectra for the most distorted sites. Thus it is difficult to obtain reliable information on the relative amounts of Al in the various oxygen polyhedra. For these reasons much care is required in the interpretation of the NMR spectra of quadrupolar nuclei. The situation is completely different for ^{29}Si (spin 1/2); there are no quadrupolar interactions, the observed chemical shifts are the isotropic ones and in some cases the different SiO_4 tetrahedra may be quantified if a correct simulation of the spectra is made and providing long enough recycle times are used.

3.3.1. Single phase precursors

The evolution of the NMR spectra of the precursor A with treatment temperature is reported on Fig. 2(a and b) This single phase precursor crystallizes into mullite at 980 °C. The ^{27}Al spectra show that at 750 °C aluminium is tetra-, penta- and hexa-coordinated. The isotropic chemical shifts, corrected for quadrupolar interactions, are respectively at 67, 37 and 6 ppm while their apparent maximum intensities are at 55, 24 and 0 ppm. In the amorphous state the relative intensities of the Al(IV) and Al(V) sites increase with temperature to the detriment of Al(VI) and they are at their maximum before the crystallization. The decrease of the amount of Al(VI) is apparent from 750–970 °C. The spectra have been simulated with quadrupolar lines [22, 23] (see example on Fig. 3). Considering that all the aluminium atoms are observed, and with caution

inherent to the quadrupolar nucleus, the powder calcined to 750 °C is estimated to contain ~10% Al(VI), while this ratio falls to ~3% at 970 °C, that is just before the crystallization. The band of each site is broadened on its high field side, so the apparent intensity of Al(VI) includes the trailing contributions of Al(V) and Al(IV). At 1000 °C the powder is crystallized in an alumina-rich mullite (Al:Si = 4:1 by XRD) and we note the presence of three Al sites according to the crystallographic data: one octahedral site at -3 ppm (apparent chemical shift) and two tetrahedral sites denoted T and T* [41, 42] with their respective chemical shifts at 60 and 44 ppm. After simulation of the central and satellite transitions, the corrected isotropic positions are at 8, 70 and 50 ppm. From 1000 °C (Al:Si = 4:1 from XRD) and 1300 °C (Al:Si = 3:2) we note an apparent increase of the Al(IV):Al(VI) ratio, which is contrary to what is expected from the variation of the chemical composition within the mullite solid solution. The formula of mullite being $Al_2^{VI}(Al_{2+2x}Si_{2-2x})^{IV}O_{10-x}$, as the silica increases, the ratio Al(IV):Al(VI) should decrease. This illustrates the difficulty in accurately determining the occupancies of the different sites. A more extended study carried out at two contrasting principal magnetic fields would give further information about this point.

The ^{29}Si spectra of the sample show, at 750 °C, a broad resonance centred at -89 ppm, traducing a quasi-random distribution of Si and Al atoms in the lattice. This resonance is shifted to high fields by increasing the temperature (-96 ppm at 900 °C). At 1000 °C the spectrum shows two resonance bands, one relative to mullite centred at -89 ppm, and the other, at -109 ppm, relative to free silica. The NMR spectroscopy clearly shows the segregation of silica during the crystallization at 980 °C. Considering that all the silicon atoms are observable by NMR, by simulation of the spectrum with Gaussian profiles one can deduce the chemical composition of the crystallized mullite. The resonance relative to the free silica represents 30% of the total amount of the silicon atoms in the analysed sample. Thus for mullite, at this temperature, the calculated atomic ratio Al:Si = 4:3 is close to that (Al:Si = 4:1) determined from the X-ray diffraction. At 1300 °C (1/2 h), the spectrum is characteristic of 3:2 mullite [41-43], with an apparent main resonance at -86.6 ppm, relative to sillimanite-type SiO_4 tetrahedra, and other peaks or shoulders at -80, -90 and -94 ppm. However some free silica still remains (6% of the total Si). The sample is thus slightly richer in alumina than the $3Al_2O_3 \cdot 2SiO_2$ mullite. The same ratio Al:Si = 3:2 is found by NMR and XRD. There

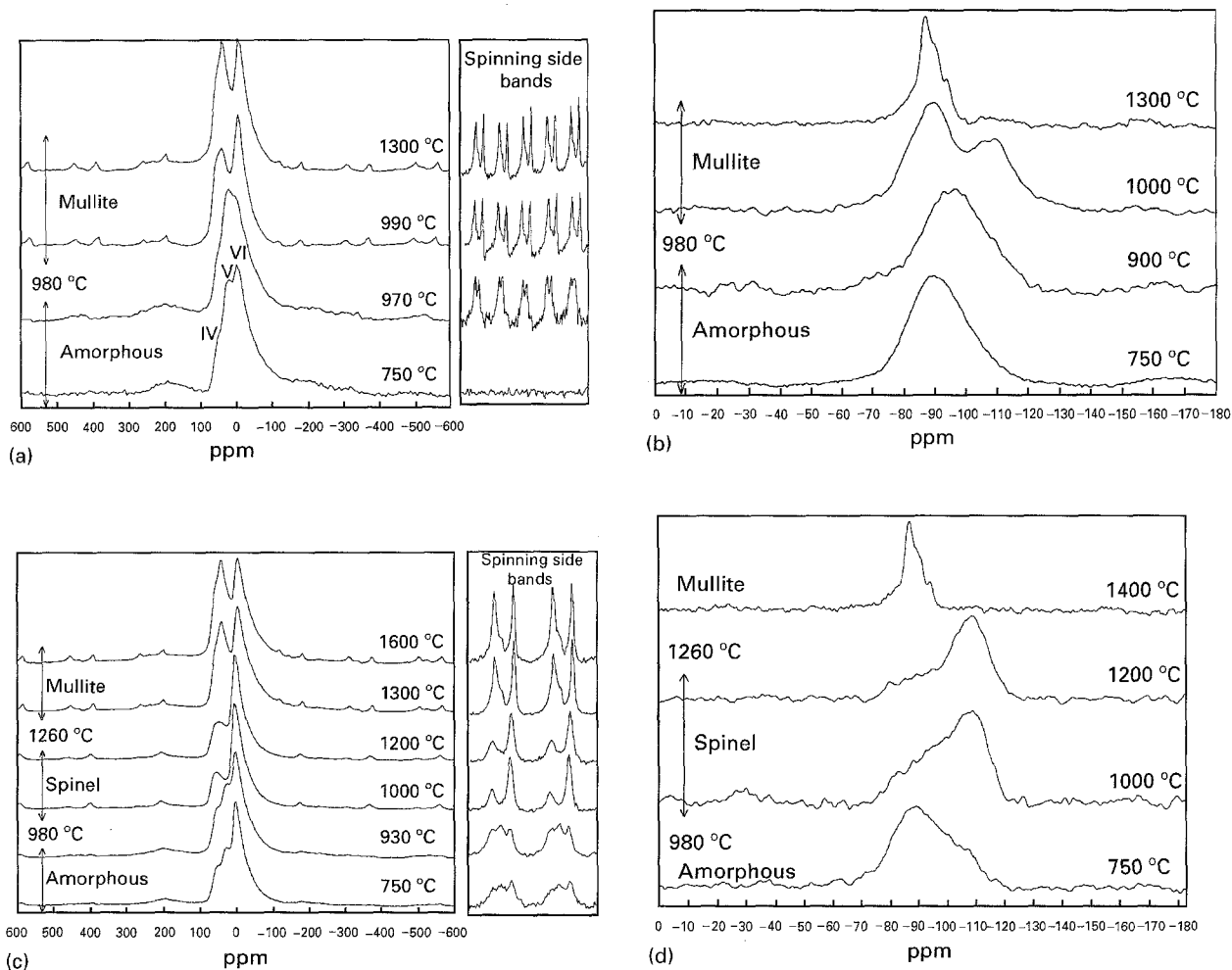


Figure 2 (a) ^{27}Al and (b) ^{29}Si MAS-NMR spectra for monophasic sample A, (c) ^{27}Al and (d) ^{29}Si MAS-NMR spectra for diphasic sample B, (e) ^{27}Al and (f) ^{29}Si MAS-NMR spectra for monophasic sample C, (g) ^{27}Al and (h) ^{29}Si MAS-NMR spectra for diphasic sample D and (i) ^{27}Al and (j) ^{29}Si MAS-NMR spectra of monophasic sample E. The data were acquired at room temperature after heat treatments at the given temperatures.

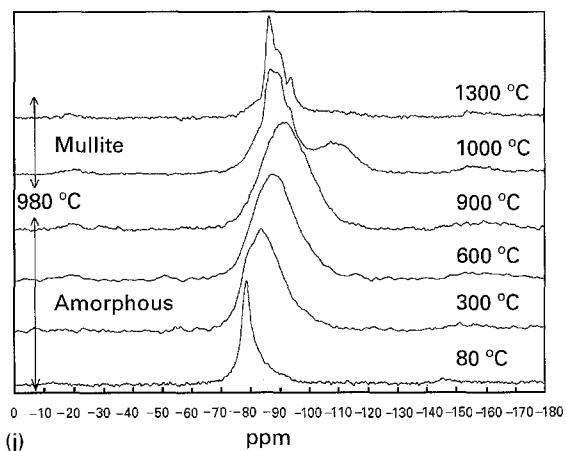
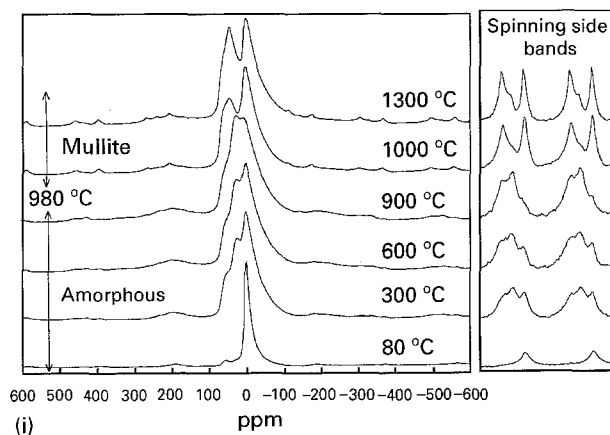
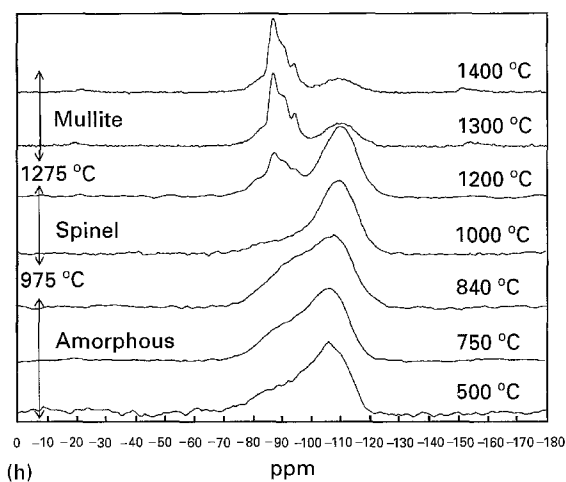
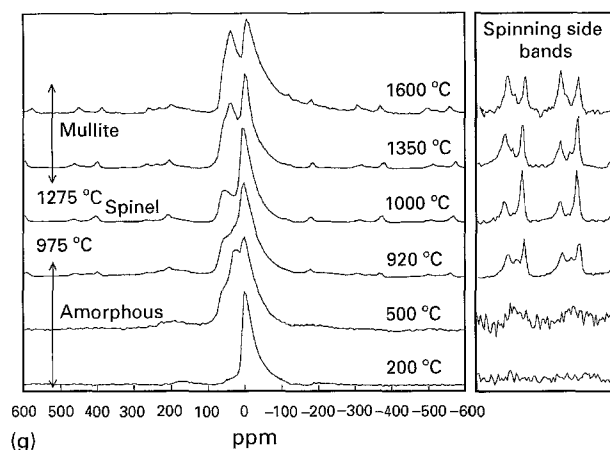
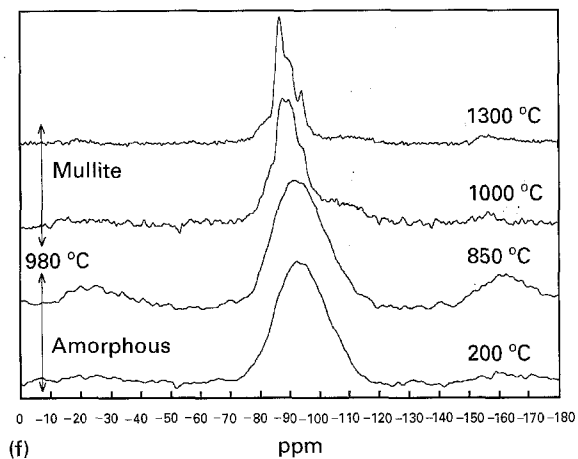
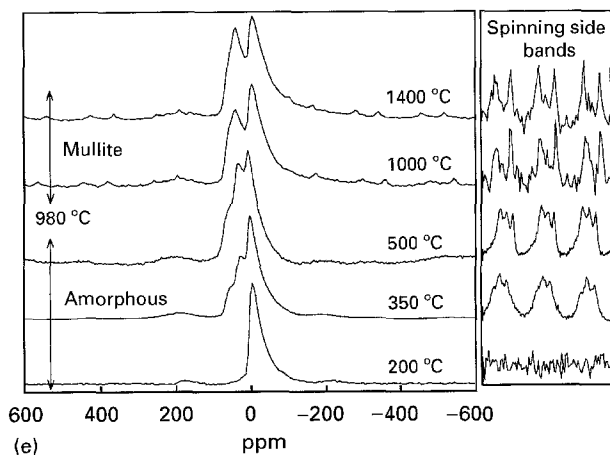


Figure 2 Continued.

is a good agreement between the two techniques in the determination of the chemical composition.

The structural evolutions are very similar for the single phase precursors C, spray-dried powder Fig. 2(e and f) and E, precipitated gel Fig. 2(i and j). In sample C, just spray-dried, Al is present as Al(VI). At this stage, aluminium nitrate is not yet decomposed. By heating the precursor, the bands corresponding to Al(IV) and Al(V) increase while Al(VI) decreases. For sample E, dried at 100 °C, the local structure is that of protoimogolite allophane [31], with a single environment at -78 ppm for the silicon atoms and practi-

ally all the aluminium atoms being hexacoordinated. Each silicon is linked to three Al(VI) by bridging oxygens and to one hydroxyl group. At 300 °C this structure is completely lost and the evolution is that of usually single phase precursors.

3.3.2. Diphasic precursors

The evolution of the environments for Al and Si atoms in the diphasic precursors B(Fig. 2(c and d)) D(Fig. 2(g and h)) is different. Sample B crystallizes into spinel at 980 °C and mullite at 1260 °C. As for single phase

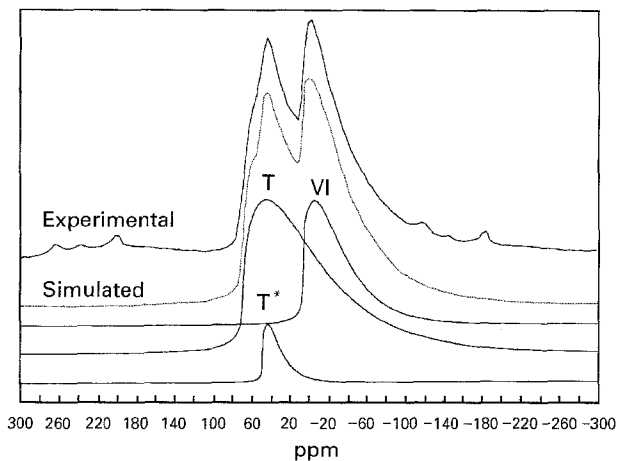


Figure 3 Example of ^{27}Al NMR spectrum simulated by quadrupolar bands.

precursors, ^{27}Al spectra show, in the amorphous state, an increase of the tetra- and pentahedral sites to the detriment of Al(VI). However the main difference is in the amount of residual hexa-coordinated aluminium atoms before the crystallization. For the sample B at 930°C this is estimated as 18% while for A it falls to a very low level (3%). The situation is then closer to that in pure amorphous alumina precursors. In two alumina precursors, obtained by spray-drying a solution of aluminium nitrate and by homogeneous precipitation (not reported here), Al(VI), largely predominant at low temperatures, decreases to $\sim 24\%$ at $400\text{--}500^\circ\text{C}$ and increases again to $\sim 31\%$ before crystallizing into $\gamma\text{-Al}_2\text{O}_3$ at respectively 865°C and 820°C . A similar evolution has been reported by Wood *et al.* [27]. The ^{27}Al spectra at 1000°C and 1200°C are similar to that of $\gamma\text{-Al}_2\text{O}_3$. When the treatment temperature increases the Al(IV):Al(VI) ratio increases in the spinel phase. At 1300°C the spectrum is characteristic of mullite [44, 45]

The ^{29}Si spectra of this sample (Fig. 2d) are different from those of homogeneous precursors. At 750°C the resonance is broad and asymmetric. It can be resolved into two bands, one centred on -89 ppm relative to an aluminosilicate network and the other, at -105 ppm, relative to silica. The NMR spectroscopy shows a segregation in this sample. The respective atomic populations are 82% and 18%. At 1000°C only spinel is crystallized. The ^{29}Si spectrum may be decomposed into two lines, centred on -95 ppm for the crystalline spinel, and on -108 ppm for the free silica, with respectively 60% and 40% of the silicon atoms. The chemical composition of the spinel phase may thus be estimated to be 71.4 mol% Al_2O_3 and 28.6% SiO_2 , with an atomic ratio Al:Si = 5:1. At 1200°C the spectrum is similar, but the respective amounts of silicon atoms in spinel and silica are now 30 and 70%, corresponding to an atomic ratio Al:Si = 10:1 or a composition of 83 mol% Al_2O_3 /17 mol% SiO_2 . Therefore, between $1000\text{--}1200^\circ\text{C}$, silica continues to be segregated and the spinel phase becomes richer in alumina. At 1400°C the spectrum is that of orthorhombic mullite.

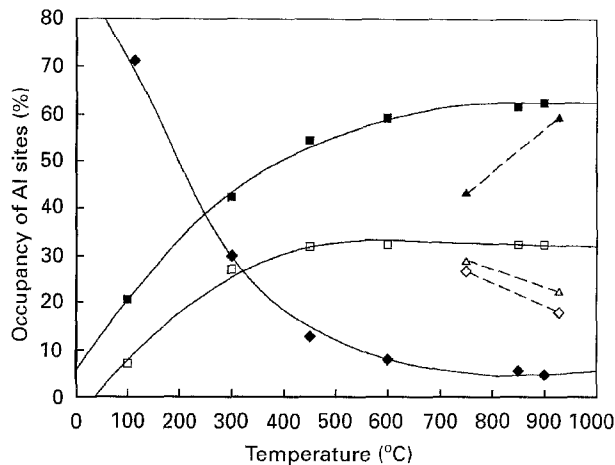


Figure 4 Variation of the estimated occupancies of (■) AlO_4 , (□) AlO_5 and (◆) AlO_6 polyhedra in monophasic (E) precursor and variation of the estimated occupancies of (▲) AlO_4 , (△) AlO_5 and (◇) AlO_6 in a diphasic (B) precursor with the heat treatment temperature.

Precursor D has been obtained by spray-drying a suspension of colloidal silica in a solution of aluminium nitrate. It crystallizes into spinel and a small amount of mullite at low temperature. Mullite is completely crystallized at 1275°C . The ^{29}Si NMR resonance at 500°C (Fig. 2h) is broad and asymmetric like for B, and may be simulated by two bands centred at -93 and -108 ppm. The latter, relative to free silica, increases regularly from the amorphous to spinel, representing 50, 52, 54 and 60% of the silicon atoms from $500\text{--}1000^\circ\text{C}$. At 1200°C the amorphous silica still contains 62% of the Si atoms and mullite is clearly identified. At 1300 and 1400°C , after the transformation of spinel into mullite, a small amount of free silica is still present in the sample.

3.3.3. Mullite or spinel?

For amorphous diphasic precursors, the segregation of silica is evidenced by a ^{29}Si NMR contribution at ~ -110 ppm, while this is absent for single phase precursors. For the former, the chemical composition of the aluminosilicate phase is thus richer in alumina and a crystallization into spinel will result. The other difference, denoted by ^{27}Al NMR spectroscopy, lies in the occupancies of the different polyhedra by the aluminium atoms. Fig. 4 shows the evolutions of these occupancies with the temperature for a single phase (E) and a diphasic (B) precursors. The values are estimated due to the difficulties of handling a quadrupolar nucleus. All the spectra were simulated with the same parameters and thus the most important feature is the comparative evolutions. For a chemically homogeneous sample Al(IV) is predominant at temperatures higher than 300°C . Al(V) is also present while Al(VI) decreases to a very low value at high temperatures. For the diphasic precursor B, Al(IV) is also the major form before the crystallization while Al(VI) remains at a higher level. The NMR spectroscopy shows that the crystallization scheme is related

to the structural short-range order in the non-crystalline precursors.

A general trend in aluminosilicates is the increase of Al(VI) when the alumina content increases [30, 46–48]. The effect of temperature is contrary. For a $3\text{Al}_2\text{O}_3 \cdot 2\text{SiO}_2$ single phase precursor, with a chemical homogeneity at the atomic level, when the temperature approaches 980°C , Al(IV) is maximum, Al(VI) is at a low level and mullite crystallizes. For a diphasic precursor of the same global composition, silica is segregated, thus the local composition in the aluminosilicate phase is richer in alumina, the short-range order is closer to that of pure Al_2O_3 precursor with a higher content in Al(VI) and spinel crystallizes. This is consistent with the results of Okada and Otsuka [13] who studied the crystallization for monophasic and diphasic gels of different compositions in the alumina–silica system.

Huling and Messing [16] have clearly shown the enhancement of spinel nucleation in aluminosilicate gels. Even a few wt % segregated alumina are sufficient for spinel to dominate crystallization at $\sim 1000^\circ\text{C}$. In the absence of evidence of segregated alumina, but when free silica is observed by NMR spectroscopy, the aluminosilicate regions are richer in alumina and the modified short-range order is more favourable for spinel nucleation and crystallization.

4. Conclusion

^{29}Si and ^{27}Al MAS NMR spectroscopy has been used to investigate the short-range structural evolution of the different precursors from the amorphous state to mullite. Complementary information about crystallization has been obtained from XRD and DSC analyses. Good agreement is found in the determination of the chemical composition of non-stoichiometric 3:2 mullites by two different techniques: XRD and ^{29}Si NMR spectroscopy.

Single phase precursors, with the $3\text{Al}_2\text{O}_3 \cdot 2\text{SiO}_2$ composition, crystallize into an alumina-rich mullite $2\text{Al}_2\text{O}_3 \cdot \text{SiO}_2$ at 980°C through a strong exothermic reaction. An enthalpy of crystallization of ~ 75 kJ per mol is determined for the 2:1 mullite. By further heating the silica expelled during the crystallization progressively re-enters the mullite lattice, and the stoichiometric composition of the 3:2 mullite is reached at $\sim 1300^\circ\text{C}$.

For diphasic (or type III) precursors, the NMR spectroscopy shows the segregation of silica in the non-crystalline state. These precursors crystallize into spinel at $\sim 980^\circ\text{C}$ through a weaker exotherm. The crystallized phase is also richer in alumina than the parent amorphous phase since the amount of free silica increases. The alumina content increases on increasing the temperature in the spinel phase until a second exotherm at 1260 – 1275°C , when spinel reacts with silica to yield the 3:2 mullite.

The nature of the crystallization depends on the short-range order around the aluminium atoms. In single phase precursors the hexacoordinated atoms practically completely disappear before 980°C and mullite crystallizes. In diphasic precursors the

aluminosilicate phase has a higher content in AlO_6 octahedra, resulting in the crystallization of spinel.

Acknowledgements

We acknowledge financial support from CNRS and Région Centre.

References

1. I. A. AKSAY, D. M. DABBS and M. SARIKAYA, *J. Amer. Ceram. Soc.* **74** (1991) 2343.
2. M. D. SACKS, H. W. LEE and J. A. PASK, in Ceramic Transactions, Vol. 6, "Mullite and Mullite Matrix Composites" edited by S. Somiya, R. F. Davis and J. A. Park (The American Ceramic Society, Westerville, OH 1990) p. 167.
3. D. W. HOFFMAN, R. ROY and S. KOMARNENI, *J. Amer. Ceram. Soc.* **67** (1984) 468.
4. H. SCHNEIDER, B. SARUHAN, D. VOLL, L. MERWIN and A. SEBALD, *J. Eur. Ceram. Soc.* **11** (1993) 87.
5. J. LIVAGE, M. HENRY and C. SANCHEZ, *Progress in Solid State Chemistry* **18** (1988) 259.
6. C. J. BRINKER and G. W. SCHERER "Sol-Gel Science. The Physics and Chemistry of Sol-Gel Processing" (Academic Press, San Diego, CA, 1990).
7. P. COLOMBAN, *J. Mater. Sci.* **24** (1989) 3011.
8. B. E. YOLDAS and D. P. PARTLOW, *Ibid* **23** (1988) 1895.
9. C. SANCHEZ, J. LIVAGE, M. HENRY and F. BABONNEAU, *J. Non-Cryst. Solids* **100** (1988) 65.
10. T. HEINRICH and F. RAETHER, *Ibid* **147 & 148** (1992) 152.
11. Y.-F. CHEN and S. VILMINOT, *J. Sol-Gel Sci. & Technol.* **2** (1994) 399.
12. I. JAYMES, A. DOUY, P. FLORIAN, D. MASSIOT and J. P. COUTURES, *Ibid* **2** (1994) 367.
13. K. OKADA and N. OTSUKA, *J. Amer. Ceram. Soc.* **69** (1986) 652.
14. D. X. LI and W. J. THOMSON, *J. Mater. Res.* **5** (1990) 1963.
15. J. C. HULING and G. L. MESSING, *J. Amer. Ceram. Soc.* **72** (1989) 1725.
16. *Idem, ibid.* **74** (1991) 2374.
17. *Idem, J. Non-Cryst. Solids* **147&148** (1992) 213.
18. A. DOUY, *J. Eur. Ceram. Soc.* **7** (1991) 117.
19. A. DOUY, in "Chemical Processing of Advanced Materials", edited by L. L. Hench and J. K. West (Wiley, New York, 1992), p. 585.
20. I. JAYMES and A. DOUY, *J. Amer. Ceram. Soc.* **75** (1992) 3154.
21. *Idem, J. Sol-Gel Sci. & Technol.* **4** (1995) 7.
22. C. JÄGER, *J. Magn. Reson.* **99** (1992) 353.
23. D. MASSIOT, B. COTE, F. TAULELLE and J. P. COUTURES, in "Applications of NMR to Cement Sciences", Edited by P. Colombet and A. R. Grimmer (Gordon and Breach, New-York, 1994) p. 153.
24. A. DOUY and P. ODIER, *Mater. Res. Bull.* **24** (1989) 1119.
25. A. KATO, K. INOUE and Y. KATATAE, *Ibid.* **22** (1987) 1275.
26. B. AIKEN, W. P. HSU and E. MATIJEVIC, *J. Amer. Ceram. Soc.* **71** (1988) 845.
27. T. E. WOOD, A. R. SIEDLE, J. R. HILL, R. P. SKARJUNE and C. J. GOODBRAKE, in *Mat. Res. Soc. Symp. Proc.* Vol. 180: "Better Ceramics through Chemistry IV" edited by C. J. Brinker, D. E. Clark and D. R. Ulrich, (The Materials Research Society, Pittsburg, PA, 1990) 97.
28. W. H. R. SHAW and J. J. BORDEAUX, *J. Amer. Chem. Soc.* **77** (1955) 4729.
29. R. K. ILLER, "The Chemistry of Silica" (Wiley, New York, 1979).
30. I. JAYMES, A. DOUY, D. MASSIOT and J. P. BUSNEL, *J. Amer. Ceram. Soc.* **78** (1995) 2648.
31. B. A. GOODMAN, J. D. RUSSEL, B. MONTEZ, E. OLDFIELD and R. J. KIRKPATRICK, *Phys. Chem. Mineral.* **12** (1985) 342.
32. W. E. CAMERON, *Amer. Mineral.* **62** (1977) 747.

33. R. X. FISCHER, H. SCHNEIDER and M. SCHMÜCKER, *Amer. Mineral.* **79** (1994) 983.
34. F. J. KLUG, S. PROCHAZKA and R. H. DOREMUS, in *Ceramic Transactions*, vol. 6, "Mullite and Mullite Matrix Composites" edited by S. Somiya, R. F. Davis and J. A. Park (The American Ceramic Society, Westerville, OH, 1990) p. 15.
35. T. BAN and K. OKADA, *J. Amer. Ceram. Soc.* **75** (1992) 227.
36. J. OSSAKA, *Nature* **19** (1961) 1000.
37. S. KANZAKI, H. TABATA, T. KUMAZAWA and S. OHTA, *J. Amer. Ceram. Soc.* **68** (1985) C-6.
38. G. ENGELHARDT and D. MICHEL, "High Resolution Solid-State NMR of Silicates and Zeolites" (Wiley, New York, 1987).
39. E. LIPPMAA, A. SAMOSON and M. MAGĪ, *J. Amer. Ceram. Soc.* **108** (1986) 1730.
40. G. L. TURNER, R. J. KIRKPATRICK, S. H. RISBUD and E. OLDFIELD, *Amer. Ceram. Soc. Bull.* **66** (1987) 656.
41. L. H. MERWIN, A. SEBALD, R. RAGER and H. SCHNEIDER, *Phys. Chem. Minerals* **18** (1991) 47.
42. H. SCHNEIDER, L. MERWIN and A. SEBALD, *J. Mater. Sci.* **27** (1992) 805.
43. T. BAN and K. OKADA, *J. Amer. Ceram. Soc.* **76** (1993) 2491.
44. J. SANZ, I. SOBRADOS, A. L. CAVALIERI, P. PENA, S. de AZA and J. S. MOYA, *Ibid.* **74** (1991) 2398.
45. G. KUNATH-FANDREI, P. REHAK, S. STEUERNAGEL, H. SCHNEIDER and C. JÄGER, *Solid State Nucl. Magn. Reson.* **3** (1994) 241.
46. S. KOMARNENI, R. ROY, C. A. FYFE, G. J. KENNEDY and H. STROBL, *J. Amer. Ceram. Soc.* **69** (1986) C-42.
47. A. D. IRWIN, J. S. HOLMGREN and J. JONAS, *J. Mater. Sci.* **23** (1988) 2908.
48. S. L. HIETALA, D. M. SMITH, C. J. BRINKER, A. J. HURD, A. H. CARIM and N. DANDO, *J. Amer. Ceram. Soc.* **73** (1990) 2815.

*Received 21 March 1995
and accepted 18 March 1996*